We are IntechOpen,
the world's leading publisher of Open Access books
Built by scientists, for scientists

6,900
Open access books available

185,000
International authors and editors

200M
Downloads

154
Countries delivered to

Our authors are among the

TOP 1%
most cited scientists

12.2%
Contributors from top 500 universities

Interested in publishing with us?
Contact book.department@intechopen.com

Numbers displayed above are based on latest data collected.
For more information visit www.intechopen.com

Chapter

Enhancing Surface Heat Transfer Characteristics Using Laser Texturing

Nickan H. Ghahramani, Martin Sharp, Michael Morgan and Mehdi Seddighi

Abstract

The use of a pulsed laser system to manufacture parallel streamwise riblets on the plates of a heat exchanger is reported. There are certain laser system elements that can influence the quality of a micrometre texture geometry; among these, there was a focus on laser incubation effect on obtaining greater depth of the riblets. Surface roughness was always considered to keep the heat transfer efficiency high. The heat exchanging process was measured in two flow regimes: laminar and turbulent. In laminar flow, the surface texture slightly deteriorated the heat transfer rate. However, small improvement in the heat transfer rate was observed in turbulent flow.

Keywords: heat transfer, laser texturing, drag reduction

1. Introduction

Many engineering designs have been inspired by nature. The surface traits of lotus leaf and shark skin are examples of biology being mimicked to inspire designs. Lotus leaves have hierarchical superhydrophobic behaviour which enables the water droplets to roll off and clean the surface by rubbing the dirt particles. The skin of fast swimming sharks is covered with streamwise dermal denticles which have been shown to reduce drag plus having the anti-microorganism fouling feature.

The effect of textures on fluid flow behaviour have been widely studied for drag reduction purposes, more specifically for improving aerodynamic behaviour of solid structures such as aeroplane air foils. The results indicate a considerable drag reduction of approximately 10% compared with a conventional design, successful in creating a more innovative surface design.

Skin drag reduction can also have positive effects on lowering energy consumption in automotive, offshore, and marine industries. There are numerous methods of skin drag reduction such as using wavy surfaces and riblets. Riblets are streamwise parallel patterns whose shape optimization is still in progress.

Skin drag reduction can also improve the efficiency of heat transfer on surfaces dealing with heat transfer. There has not been significant research in this area. Nishida et al. [1] demonstrated the effect of wavy surfaces on heat transfer improvement.

Most studies have been considering the theoretical effects of drag reduction regardless of manufacturing techniques. This project focused on texturing the surface of stainless-steel plates of a heat exchanger by pulsed laser ablation to obtain scalloped riblet design with increased groove depth suggested by Bechert et al. [2].

2. Literature review

Turbulent and Laminar regimes of a flow depend on the relative importance of fluid viscosity (friction) and flow inertia. In turbulent flow the molecules of the fluid move in swirling and cross-stream directions while maintaining the average velocity in the fluid direction.

In turbulent flow around a flat plate, the vortices dominate the area in the viscous layer and the interaction between these vortices and the wall increases the shear stress on the wall causing a rise in the drag factor.

2.1 Drag reduction study

Drag reduction by using textured surfaces has been widely considered in recent studies. Examples in the nature can be used as the best samples for industrial applications. Lotus leaves have natural traits that possess a hierarchical surface structure which leads to a super-hydrophobic behaviour. Another example is Rose petals with super-hydrophobicity and either high or low adhesion [3].

The mucus of fish skin causes a drag reduction and protects the fish from abrasion. The dermal denticles of shark skin are shaped like streamwise riblets that reduces drag up to nearly 10% [2]. The magnitude of drag can be reduced by creating streamlined shapes as the viscous drag is created by the interactions between the molecules of the fluid and a surface parallel to the flow. By moving away from the surface, the flow reaches the mean velocity.

The outer layers of the turbulent boundary layer are disorganised due to the streamwise vortices forming on the surface of the viscous sub-layer. The interaction between the vortices and the surface causes vortices to get ejected from the surface and moved to the outer boundary layers. Reducing this bursting behaviour of such streamwise vortices can cause drag reduction [4].

2.2 Riblets in drag reduction

The first hypothesis on drag reduction was that the surface would redistribute the shear stress with concentration at the protruding parts of the surface. A better explanation is that longitudinal ribs rectify the turbulent flow in streamwise direction and reduce the turbulent momentum transfer close to the surface and hence decrease the shear stress.

Riblets on the skin of a fast-swimming shark reduce the occurrence of vortex ejection and the momentum transfer by impeding the vortex translation in the outer boundary layer. In turbulent flow, fluid drag increases with an increase in wetted surface area due to the shear stress actions. The low velocity fluid in the valleys of the riblets produce very low shear stress across the surface of the riblets and by keeping the vortices above, cross-stream velocity fluctuations between the riblet valleys and above the flat plate increases which is due to the reduction in shear stress and momentum transfer near the surface.

Riblets can reduce the cross-stream translation by protruding into the flow without increasing the drag. As vortices start to form on the surface, they remain above the riblet tips that creates low velocity channel in the riblet valleys. These channels have lower velocity gradient than the flow over a flat plate which reduces the shear stress over the riblet surface. On the other hand, considering the higher shear stress at the riblet tips due to higher velocity gradient, the result of this shear-stress distribution reduces the overall drag.

More recent works investigated the effect of drag reduction on heat transfer using numerical modelling. Zhu et al. investigated the nature-inspired structures in this field [5]. Soleimani and Eckels obtained benefit of riblets to drag reduction in a circular closed channel [6]. However, lack of experimental data to validate the result is still prominent in most works. This experimental research aimed to contribute to the field through an experimental study by employing laser texturing.

2.3 Effect of roughness on heat transfer

Surface roughness increases friction factors and the heat transfer coefficients within a turbulent boundary layer. In flat plate flows, ε/δ decreases along the plate, where δ is the boundary layer thickness and ε being the roughness height [7].

The relative effect of roughness is determined by roughness Reynolds number as follows:

$$Re_k = \frac{u_\tau \varepsilon}{v} \tag{1}$$

Where ε is the surface roughness, and u_τ being the friction velocity. When Re_k is less than 5, the surface is considered hydraulically smooth and for $Re_k > 70$, the flow is in the fully rough regime. For $5 < Re_k < 70$, the flow in transitionally rough regime. In turbulent flows, rough surfaces usually develop larger skin friction coefficients. In heat transfer there is the same behaviour although the skin friction increase is smaller for heat transfer. Surface roughness reduces the Reynold number for the transition from laminar to turbulent flow.

Abuaf et al. conducted an experimental study between air foils with different degrees of surface finish to measure the heat transfer coefficient shows that polishing the surface reduces the average roughness and improves the performance. However, very small differences have been observed between 0.03 and 0.81 micrometre surface roughness.

2.4 Laser texturing

Nanosecond lasers have been widely used in micro-machining and laser texturing. Etsion et al. [8] studied the possibility of reducing friction on piston rings to improve fuel efficiency in diesel engines. Gao et al. [9] investigated the possibility of increasing the smoothness of the surface through adding a second step laser ablation process.

Laser ablation Surface texturing has the advantage of contactless machining with high spatial resolution at fast speed. Among the variety of laser types, nano-second (ns) pulsed laser is widely used due to its affordability and short pulse duration which can create small heat affected zones.

Direct laser ablation (DLA) has been also used for controlling the wettability of metals by either laser texturing at low fluence near the ablation threshold fluence with polarised pulses or laser texturing at high fluence when pulse polarisation is not

important. However, direct laser texturing at high fluence has been mostly done through ultra-short pulses (fs and ps). The considerable point is that it is not possible to achieve a hydrophobic surface by adding roughness when the material is already hydrophilic [10]. Menghistu et al. [11] concluded that by keeping the textured surface at atmospheric air, hydrophobic characteristics started to develop. The transformation could not be observed when leaving the textured surface in water.

Appropriate selection of the wavelength and process energy plays an important role in machining quality of nano-second pulsed lasers. The reflectivity of metals decreases in shorter wavelengths [12]. However, the maximum laser power is directly proportioned to the wavelength. The optimum quality of laser surface finishing is achieved when the pulse energy is low; In industrial applications usually a high pulse energy is needed to remove more material. Therefore, excess interaction between the plasma and subsequent pulses should be avoided by either increasing the scanning velocity or reducing the pulse frequency.

3. Methods

Two plate-type heat exchangers were manufactured with identical dimensions, one with smooth plates and the other one with textured plates (only the plates in direct contact with hot fluid) to compare their heat transfer efficiency. The heat exchangers consist of 2 middle plates, a top covering Perspex plate, and an aluminium bed plate. The SS plates are 0.5 mm thick; gaskets are 3 mm thick. Heat exchangers were incorporated into a monitoring rig manufactured by *TecQuipment* model no. *TD-360*. The service module provides two water circuits of cold at the mean ambient temperature of 22°C and hot tank at 60°C.

The water flow can be regulated for both circuits in the range of 0–3.5 lit/min. There are temperature measurement thermocouples near the inlet/outlet hose connectors and show the temperature on the digital displays.

The cold water is from the incoming mains cold water supply which passes through a hand adjusted flow regulator valve and then enters the heat exchanger. The hot water has an electric heating tank which rises the temperature to 60°C. A supply pump then circulates the water between the tank and the heat exchanger through a regulating valve (**Figure 1**).

3.1 Surface imaging

GFM MikroCAD 3D inspection scanner was employed for surface profile measurement using structured light fringe projection profilometry. It can measure and quantify the micro-scale surface structures and geometries based on phase measuring fringe projection by digital micro mirror displays and UV-LED.

3.2 Plate machining and testing

A SPI G3 20W nS laser was used to texture the surface. Laser parameters were power 20 W, frequency 25 kHz, pulse length 200nS. The beam was steered by a Nutfield galvanometer scanning head with a 100 mm focal length f-theta lens with spot size 25 μm, and an engraving field size of 50 mm × 50 mm. This head is placed on an Aerotech 150 mm precision ballscrew slide for z-axis focus control.
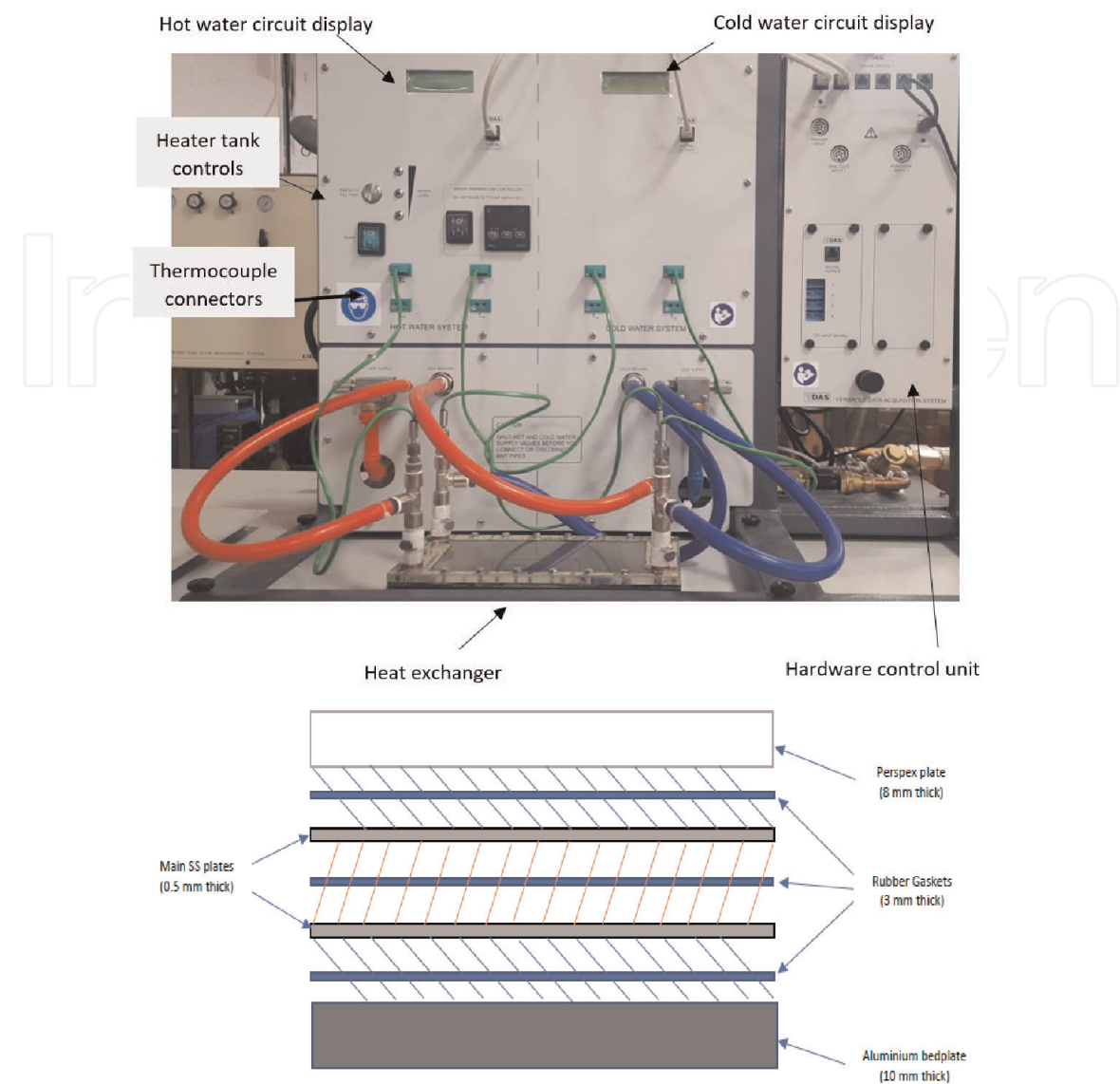
Figure 1.
Heat exchanger console and exploded side-view.

The heat exchanger plates to be engraved were mounted on a fixture mounted upon an Aerotech precision ballscrew 800 mm × 600 mm X-Y table (**Figure 2**). The levelling of the plate was checked using a dial turn indicator (DTI) attached to the z axis, while the heat transfer plate was traversed in the X and Y axes.

The riblet texture was laser engraved by using the galvanometer head to scan the focused laser beam along the parallel lines within the 50 mm × 50 mm field of the head. Upon completion of one patch of the riblets, the X-Y table was used to reposition the heat exchanger plate and the engraving process was repeated, **Figure 3**. By this means the necessary area of the plate was fully engraved with the riblet texture.

4. Heat exchanger parameters calculations

Hydraulic diameter is the ratio of cross-sectional to the wetted perimeter of the channel. For a rectangular channel where the height (b) is much smaller than the width (W) is (**Tables 1** and **2**):
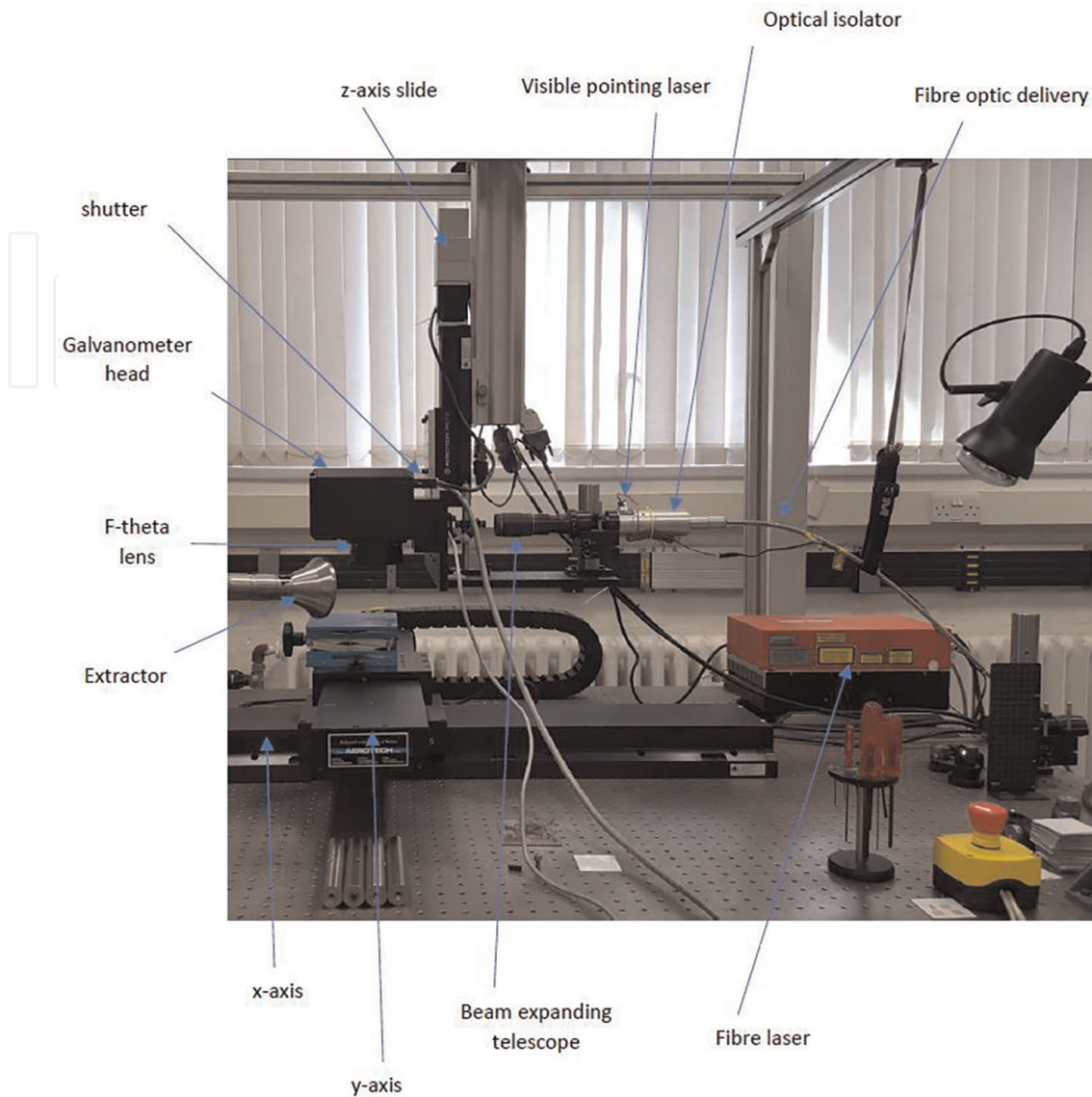
Figure 2.
Heat transfer plate mounted on table and undergoing laser machining.

$$D_H = 2b = 2 \times 0.003 = 0.006 \text{ m} \tag{2}$$

Mean temperature efficiency is defined as:

$$\bar{\eta} = \frac{\eta_H + \eta_C}{2} \tag{3}$$

Where and T_{H1} = hot in; T_{H2} = hot out; T_{C1} = cold in and T_{C2} = cold out; Accordingly $\eta_H = \frac{T_{H1} - T_{H2}}{T_{H1} - T_{C1}} \times 100$ and $\eta_C = \frac{T_{C2} - T_{C1}}{T_{H1} - T_{C1}} \times 100$.

Heat transfer emitted rate is defined as:

$$Q_e = m_h C_{ph} \Delta T_h \tag{4}$$

Where m is the mass flow rate in $\frac{Kg}{s}$; C_p is the specific heat capacity in $\frac{J}{Kg}$°K and ΔT is the temperature difference between the inlet and outlet fluid in K.
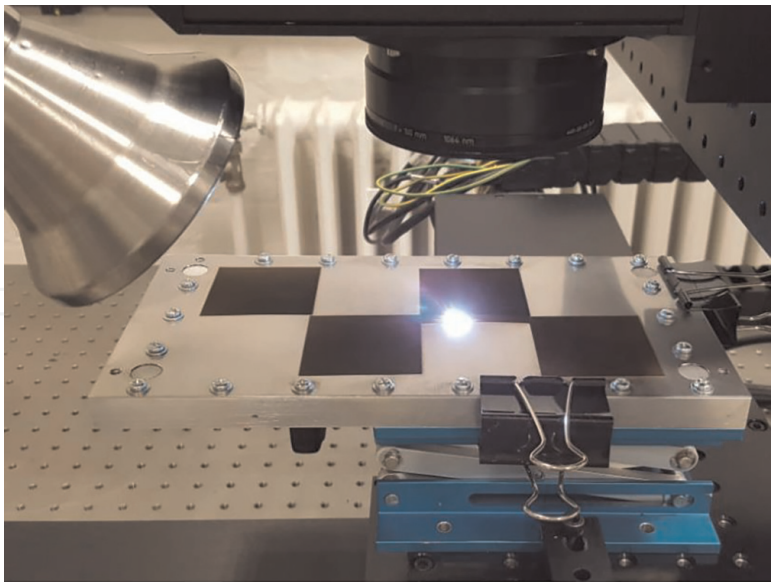
Figure 3.
Heat transfer plate mounted on table and undergoing laser machining.

Property	Unit	Hot water at 60°C	Cold water at 22°C
Heat capacity Cp	J/kg K	4190	4180
Thermal conductivity K	W/mK	0.65	0.598
Density ρ	kg/m^3	983	998
Dynamic viscosity μ	Pa s	4.6×10^{-4}	0.0010518
Flow area A = NWb	m^2	0.0003	0.0006

Table 1.
Water properties.

Property	Unit	Laminar	Turbulent
Mass flow rate m	kg/s	0.0583	0.025
Flow velocity $v = \frac{m}{A\rho}$	m/s	0.198	0.084
Reynolds number $Re = \frac{\rho v D_H}{\mu}$	—	2580	1086

Table 2.
Flow properties.

Logarithmic Mean Temperature Difference (LMTD) is the logarithmic average of the temperature difference between the hot and cold fluids and is a measure of the heat driving force which causes the heat transfer. LMTD is used when the temperature difference varies within the heat exchanger and reflects the difference more accurately.

$$LMT = \frac{(T_{H1} - T_{C2}) - (T_{H2} - T_{C1})}{\ln \left(\frac{T_{H1} - T_{C2}}{T_{H2} - T_{C1}} \right)} \tag{5}$$

Heat transfer coefficient measures the heat exchanging rate of the wall and boundary layers. The higher this coefficient, the more efficient the system is.

$$U = \frac{Q_e}{A \times LMTD} \tag{6}$$

Where Q_e is the energy emitted and $A =$ the heat exchange area

4.1 Plates' surface geometry calculations

Turbulence level scales on the shear and the shear strength is represented by a velocity scale classed shear velocity which characterises the shear at the boundary.

$$u_\tau = \sqrt{\frac{\tau}{\rho}} \tag{7}$$

Where τ is shear stress. Friction coefficient derived from Moody graph [13] equals to 0.03 with Reynolds number of 2580 for the hot chamber. Friction coefficient is defined as:

$$C_f = \frac{\tau}{\frac{1}{2}\rho u^2} \tag{8}$$

Where u is the flow velocity of the hot chamber in m/s. Therefore, the wall shear stress can be calculated as $\tau = 0.03 \times 0.5 \times 983 \times 0.198^2 = 0.578$. Using Eq. (7), friction velocity (shear velocity) would be $u_\tau = 0.024 \, m/s$. The shape of velocity profile within a turbulent boundary later has specific characteristics close to the bed where viscosity controls the vertical transport of momentum. The region is called the "viscous sublayer" where turbulence is suppressed by viscosity. The profile shape depends on friction velocity and bed texture described by the roughness. The thickness of viscous sublayer is:

$$\delta_s = \frac{5\upsilon}{u_\tau} \tag{9}$$

Where υ is the kinematic viscosity in $\frac{m^2}{s}$ and u_τ is the shear velocity in m/s. When the surface texture is smaller than the viscous sub-layer, the flow above does not feel the texture [3]. Having kinematic viscosity of water at $60°C \, \upsilon = 4.736 \times 10^{-7} \left(\frac{m^2}{s}\right) \rightarrow \delta_s \cong 90 \, \mu m$. Therefore, the texture depth should be minimum 90 μm to have an effect on the flow. However, for optimum riblet height should be:
$10 = \delta \frac{u_\tau}{\upsilon} [2] \rightarrow \delta = 150 \, \mu m$.

5. Laser ablation

Figure 4 shows the textured geometry. The riblets are stretched in a regular pattern along the plate with average height of 90 μm which is close to the viscous sub-layer thickness and is expected to influence the flow (**Table 3**).
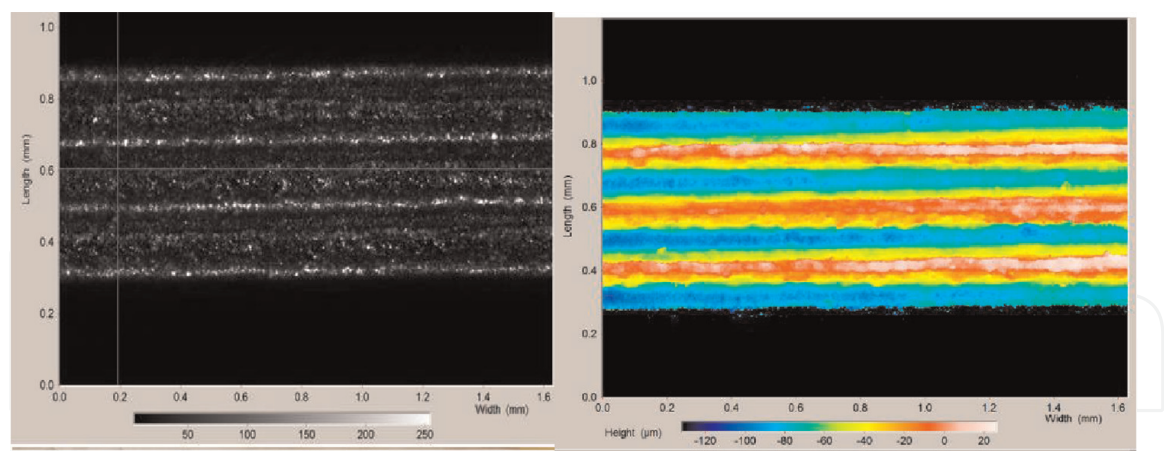
Figure 4.
Schematic display of the riblets with colour variation indicating depth of the geometry.

	Ra (μm)	Rt (μm)	Rz (μm)
Smooth plate	0.16	2.18	1.42
Textured plate (streamwise direction)	7.5	54	38
Textured plate (cross-stream) direction	24.5	103	97

Table 3.
Roughness of the plates before and after texturing.

6. Results and discussion

Two heat exchangers were tested in two separate days to get the accurate results due to the possible environmental effects. The heat exchangers were tested and compared at two flow rates of 1.5 l/m and 3.5 l/m which create Reynolds numbers of 1086 and 2580 respectively. Previous studies [14, 15] suggest that Reynolds number of greater than 2000 in plate type heat exchangers create turbulent flow.

When the working temperatures of the heat exchanger became static inlet and outlet temperature data of hot and cold fluid were collected for 300 seconds at intervals of 5 seconds (**Tables 4–6**).

Surface texture deteriorated the mean temperature efficiency and heat transfer coefficient for laminar flow. This is due to the increase in roughness of the plates which results in larger skin coefficient friction. A slight improvement in the mean temperature efficiency and heat transfer coefficient was observed in turbulent flow of

Flow regime	Plates	ΔT Hot	ΔT Cold	T_{C1}	T_{C2}	T_{H1}	T_{H2}
Laminar	Smooth	7.1	2.7	23.3	26.0	60.9	53.8
	Textured	6.9	2.8	23.3	26.1	61.0	54.1
Turbulent	Smooth	3.9	4.0	22.0	26.0	60.2	56.3
	Textured	3.8	3.9	23.2	27.1	60.1	56.3

Table 4.
Data collection of the heat exchanger in/out flow temperature.

Flow regime	Plates	η_H	η_C	$\bar{\bar{\eta}}$
Laminar	Smooth	18.9	7.2	13.03
	Textured	18.3	7.4	12.86
Turbulent	Smooth	10.2	10.5	10.34
	Textured	10.3	10.6	10.43

Table 5.
Mean temperature efficiency of the heat exchangers.

Flow regime	Plates	area	m_h	C_p	Q_e	LMTD	U
Laminar	Smooth	0.04	0.025	4190	743	32.65	569
	Textured	0.04	0.025	4190	722	32.81	550
Turbulent	Smooth	0.04	0.0583	4190	952	34.25	695
	Textured	0.04	0.0583	4190	928	33.05	702

Table 6.
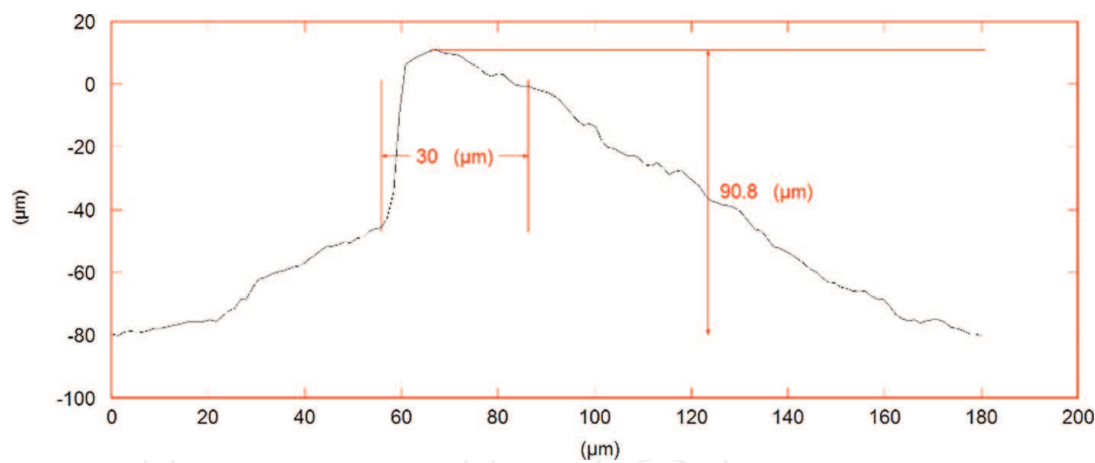*Heat transfer coefficient of the heat exchangers.*

Figure 5.
Profile depth graph of a random riblet along the path shown in black, representing a riblet pitch of 180 μm – laser machining has caused a deeper slope on one side of the riblets and a smoother curve on the other side.

the textured heat exchanger. This improvement is small, and no significant change could be concluded [16].

Machining the plates to create riblets with optimum height of 150 *μm* was not achievable using this laser set up because of the creation of high surface roughness which is not desirable for heat transfer. Moreover, deeper laser ablation could cause excess deflection of the plates. Asymmetrical geometry of riblets as a result of laser machining, could not be avoided either (**Figure 5**).

7. Conclusions

Riblets are narrow microstructures, which require very precise manufacturing methods. A 20 W nanosecond pulsed fibre laser was used towards this aim.

The texture increased the wetted surface area of the plates; nevertheless, the increase in drag reduction was not enough to predominate over the friction factor rise due to the roughness created. Manufacturing the optimum riblet height of about 150 μm could not be achieved at a reasonable timescale within this project using a 20w pulsed laser system.

The textured plates were oxidised during the laser ablation and may explain the results. Laser ablation also caused distortion of the metal. Suitable jigs and fixtures are necessary to secure the material while being machined.

The project has shown that pulsed laser machining is highly capable of producing precise geometric designs, in particular ribs of micrometre scale. While the results are not significant, the project has demonstrated enough evidence to continue to pursue this method, refining the geometry and surface condition to see if significantly higher heat transfer efficiencies can be achieved.

The overall performance of the textured heat exchanger in turbulent flow, considering the transition from laminar deterioration to turbulent slight enhancement given the undesired oxidation of the plate, was a positive indicator for further works in this field.

Acknowledgements

Author details

Nickan H. Ghahramani*, Martin Sharp*, Michael Morgan and Mehdi Seddighi*
Liverpool John Moores University, Liverpool, UK

*Address all correspondence to: hgh.info@yahoo.com; m.sharp@ljmu.ac.uk; m.seddighi@ljmu.ac.uk

IntechOpen

References

[1] Nishida A, Nakatsuji K, Hagiwara Y. Direct numerical simulation of the effects of slip velocity of wavy walls on turbulent heat transfer and drag. In: Proceedings of the 9th International Symposium on Turbulence and Shear Flow Phenomena. Danbury, USA. 2015. pp. 1-6

[2] Bechert D, Bruse M, Hage W, Van Der Hoeven J, Hoppe G. Experiments on drag-reducing surfaces and their optimization with an adjustable geometry. Journal of Fluid Mechanics. 1997;**338**:59-87

[3] Dumanis M. First course in turbulence: Dean Young. Boston Review. 1999;**24**(5):66

[4] Kline S, Reynolds W, Schraub F, Runstadler P. The structure of turbulent boundary layers. Journal of Fluid Mechanics. 1967;**30**(4):741-773

[5] Zhu Z, Li J, Peng H, Liu D. Nature-inspired structures applied in heat transfer enhancement and drag reduction. Micromachines. 2021;**12**:6

[6] Soleimani S, Eckels S. A review of drag reduction and heat transfer enhancement by riblet surfaces in closed and open channel flow. International Journal of Thermofluids. 2021;**9**:10053

[7] Abuaf N, Bunker RS, Lee CP. Effects of surface roughness on heat transfer and aerodynamic performance of turbine airfoils. In: ASME 1997 International Gas Turbine and Aeroengine Congress and Exhibition. New York, UK: American Society of Mechanical Engineers; 1997

[8] Etsion, Sher. Improving fuel efficiency with laser surface textured piston rings. Tribology International. 2009;**42**(4):542-547

[9] Gao Y, Wu B, Zhou Y, Tao S. A two-step nanosecond laser surface texturing process with smooth surface finish. Applied Surface Science. 2011;**257**(23):9960-9967

[10] Gregorčič P, Šetina-Batič B, Hočevar M. Controlling the stainless steel surface wettability by nanosecond direct laser texturing at high fluences. Applied Physics A. 2017;**123**(12):1-8

[11] Menghistu K, Sharp M. An Investigation into the Properties of Laser Machined Antifouling Microstructure. Liverpool, UK: Liverpool John Moores University; 2018

[12] Knowles M, Rutterford R, Karnakis H, Ferguson G. Micro-machining of metals, ceramics and polymers using nanosecond lasers. The International Journal of Advanced Manufacturing Technology. 2007;**33**(1):95-102

[13] Munson BR, Young DF, Okiishi TH, Huebsch WW. Fundamentals of Fluid Mechanics. Hoboken, US: John Wiley & Sons; 2014

[14] Tambe Shahanwaj K, Pandhare Nitin T, Bardeskar Santosh J, Khandekar SB. Experimental investigation of performance of plate heat exchanger for water as working fluid. International Journal of Research in Engineering and Technology (IJRET). 2015;**2015**:372-380

[15] Ayas M. Model deskového výměníku tepla. Master's thesis, Czech Technical University in Prague. Computing and Information Centre. 2015

[16] Ghahramaninia H, Sharp M, Morgan M. Heat transfer of a laser textured surface. In: Advances in Manufacturing Technology XXXIII. Amsterdam, NL: IOS Press; 2019. pp. 340-345